Industrial Crops & Products 209 (2024) 117921

Contents lists available at ScienceDirect

Industrial Crops & Products

journal homepage: www.elsevier.com/locate/indcrop

Estimation of the basic density of *Eucalyptus grandis* wood chips at different moisture levels using benchtop and handheld NIR instruments

Dayane Targino de Medeiros [a,*,1], Jhennyfer Nayara Nogueira Gomes [a,2], Felipe Gomes Batista [a,3], Adriano Reis Prazeres Mascarenhas [b,4], Emanuella Mesquita Pimenta [c,5], Gilles Chaix [d,e,f,6], Paulo Ricardo Gherardi Hein [a,7]

[a] Department Forest Science, Federal University of Lavras (UFLA), Lavras, Minas Gerais 37200–000, Brazil
[b] Department of Forest Engineering, Federal University of Rondônia (UNIR), Rolim de Moura, Rondônia 76940–000, Brazil
[c] LD celulose, Indianópolis, Minas Gerais 38490–000, Brazil
[d] CIRAD - UMR AGAP Institut, Montpellier, France
[e] UMR AGAP Institut, Univ Montpellier, CIRAD, INRAE, Institut Agro, Montpellier, France
[f] ChemHouse Research Group, Montpellier, France

ARTICLE INFO

Keywords:
Fiber saturation point
Pulp and paper industry
Multivariate statistics
Quality control
Real-time evaluation

ABSTRACT

With the increasing demand for productivity and quality in the forestry sector, near-infrared (NIR) spectroscopy is promising in the monitoring of wood properties, such as density. However, most predictive models are based on spectra acquired in wood at equilibrium moisture content using benchtop equipment. The objective of this study was to evaluate the performance of the NIR instruments in predicting the basic density of *Eucalyptus grandis* wood at different moisture contents. The wood chips were evaluated from saturated conditions (freshly felled) to hygroscopic equilibrium conditions using benchtop and portable NIR instruments. Principal component analysis (PCA) was performed to verify the behavior of spectral data, partial least squares discriminant analysis (PLS-DA) to classify density categories, and partial least squares regression (PLS-R) to develop predictive models. The moisture gradient was not the limiting factor for the statistical modeling. PCA discriminated 99.50% of the variation in the data, while the PLS-DA correctly categorized in the range of 0–94% the density classes. The models developed by PLS-R with the benchtop instrument showed a prediction coefficient (R^2) ranging from 0.79 to 0.85 and those with the portable instrument ranged from 0.77 to 0.82; the ratios of prediction deviation (RPD) were 2.20 and 2.45, respectively. Thus, NIR spectroscopy has shown potential application in wood under saturated conditions, regardless of the type of instrument. In the industrial context, the use of a portable NIR instrument could streamline wood characterization without the need for drying and transporting samples to the laboratories.

1. Introduction

Eucalyptus wood is the main source of short fibers in the pulp and paper industry. In addition, because it is versatile, *Eucalyptus* wood is a raw material widely used in the production of charcoal, reconstituted panels, furniture, and sawn wood (IBÁ, 2022). The properties of the raw materials are routinely evaluated by the industries to standardize the quality of their products, especially density, as it is a property that has a direct correlation with the physical-mechanical characteristics of the wood, with direct implications for the behavior, processing, application

* Corresponding author.
E-mail address: dayanemedeirost@gmail.com (D.T. Medeiros).
[1] ORCID: 0000–0002-1255–572X
[2] ORCID: 0000–0003-1495–7017
[3] ORCID: 0000–0002-0210–7026
[4] ORCID: 0000–0002-7554–3590
[5] ORCID: 0000–0001-5353–3132
[6] ORCID: 0000–0003-2015–0551
[7] ORCID: 0000–0002-9152–6803

https://doi.org/10.1016/j.indcrop.2023.117921
Received 5 October 2023; Received in revised form 2 December 2023; Accepted 7 December 2023
Available online 21 December 2023

and transport of the wood (Costa et al., 2019; Amaral et al., 2020). For these analyses, the technologies used are desired to be fast and effective for optimizing their production processes as opposed to conventional methods for determining the properties of wood, which are time-consuming and expensive (Medeiros et al., 2023). For this reason, the use of technologies for wood selection and monitoring is an alternative to increase the efficiency of wood production (Arriel et al., 2019).

Near-infrared (NIR) spectroscopy is a technology based on the intensity of absorption of electromagnetic radiation to analyze the interaction of biological material with the organic bonds constituting the sample. This technique has been used in the forestry sector because it is non-destructive, reliable, and provides real-time responses (Sheppard et al., 1985; Ramalho et al., 2018). The information obtained from NIR spectroscopy is associated with the values of the properties determined in the laboratory. From this, statistical models can be developed to predict such properties; partial least squares regression (PLS-R) is the most commonly used model for analysis (Sandak et al., 2016; Amaral et al., 2021).

Among the wood properties, the density variation has a strong correlation with the spectral signature in the NIR (Hein et al., 2009). In the studies by Rosso et al. (2013), Costa et al. (2018), Arriel et al. (2019), and Amaral et al. (2021), models for estimating the basic density of *Eucalyptus* wood by NIR spectroscopy with a benchtop instrument showed adequate results for the selection of the genetic material in forestry companies.

However, most of the developed models are based on wood at equilibrium moisture content with the environment (~12% dry mass basis); this content varies depending on the region. The NIR application in wood samples with different moisture gradients is important to provide technically viable equipment for real situations, such as in the field, patio, or mat, where the moisture of the wood is not controlled. Since studies regarding this aspect are scarce and a gap in scientific knowledge exists, these aspects can potentially indicate a limitation of the use of NIR in adverse conditions.

Therefore, considering hypotheses such as the independence of basic density estimation from moisture content, the comparable precision between portable and benchtop devices, and the influence of wood anatomical planes on spectra, this study aims to evaluate whether moisture content affects basic density estimation, determine if portable and benchtop devices provide equivalent precision, and investigate the impact of wood anatomical planes on the spectral analysis of *Eucalyptus grandis* wood.

2. Material and methods

2.1. Sample collection and preparation

Eucalyptus grandis tree cultivated in 3 × 3 m spacing at 33 years of age from the experimental plantation at the Federal University of Lavras (Latitude: 21° 14' 30'' S; Longitude: 44° 00' 10'' W; Altitude: 919 m) was cut following the sampling recommendations provided in ASTM 5536 (ASTM Standard, 2017a). Next, the stems with a commercial height of 26 m were sectioned to obtain eight discs in different longitudinal positions (0%, DBH (1.30 m), 15%, 30%, 45%, 60%, 75%, and 80%) for wood chip making.

A central (diametral) wood portion of each disc, comprising heartwood and sapwood, was removed with a band saw to manually produce wood chips with dimensions of approximately 30 × 30 × 4 mm (length × width × thickness). Chips were produced tangentially to the growth rings by hand using a chisel and mallet. The radial chips were made with the disc wedges, totaling 272 specimens (108 tangential + 164 radial). The chips were identified with a pencil according to the trees, disk, and position from which they were removed to represent the complete variability of the sampled trees.

2.2. Determination of basic density

The basic density was determined according to the ASTM D2395 standard (ASTM Standard, 2017b). The mass was obtained on an analytical scale (accuracy of 0.001 g), and the volume was measured using the immersion method. Next, measurements were acquired via portable and benchtop NIR spectrometers. The specimens were placed on trays for air drying in a controlled environment at 25 °C and a relative humidity of approximately 60% until the samples reached the equilibrium humidity (~12% dry basis). At each 10% moisture loss, which was monitored by constant weighing, the acquisition of mass and spectra in the chips was performed (Fig. 1), with each measurement corresponding to a drying stage, totaling 10 stages, with the last stage referring to the anhydrous mass. After reaching equilibrium moisture content, the samples were placed in an oven with a temperature adjustment of 103 ± 2 °C until the dry mass was obtained.

2.3. NIR Spectral acquisition

The spectra were collected directly on the chip surface using benchtop and portable NIR instruments. The benchtop instrument was a Fourier transform (FT) NIR spectrometer (MPA, Bruker Optik GmbH, Ettlingen, Germany) with its software OPUS v. 7.0. The spectra were recorded by diffuse reflection from the integration sphere. The spectral range used for the calculations was 1112–2500 nm (9000–4000 cm^{-1}) with a resolution of 8 cm^{-1}, resulting in 1300 spectral variables. Sixteen (16) scans were performed on each wood chip, and then the averages were calculated and compared with the standard to obtain the absorption spectrum of the specimen. Background compensation was performed every 10 min of spectral acquisition and the light leaking from the MPA window was protected.

The portable instrument was an On-site MicroNIR (Viavi Solutions Inc., CA, United States); it was directly set in reflectance mode on the surface of the wood chip. The acquisition range was from 950 to 1650 nm (10526–6060 cm^{-1}) with a resolution of 5.6 nm, with the generation of 125 spectral variables. Each spectrum had an average of 16 scans.

Using the point-and-shoot technique, a dark scan and a reference scan were performed approximately every 10 min, and the data was collected using the software SpectralSoft Solutions (Viavi Solutions Inc., CA, USA).

A total of 2720 spectra were collected on each piece of equipment, in the benchtop NIR instrument and the portable NIR instrument. The NIR data were associated with the wood density data, and multivariate models were developed.

2.4. Multivariate data analysis

The spectral data were analyzed by multivariate statistics in their original form and with mathematical treatment. Unscrambler v.9.7 software (Camo Software, NJ, USA) was used to perform principal component analysis (PCA) and partial least squares regression analysis (PLS-R). PCA was applied to analyze the grouping of the data according to the wood surfaces and the drying stages, while PLS-R was performed to develop the models for predicting the basic density of the wood by cross-validation (*leave-one-out*) and independent validation (*test set*).

For this purpose, eight latent variables were used to compare the results, and for cross-validation, the data selection method was randomized with eight segment numbers. In the *test set*, the spectra were separated into calibration and validation sets, using 60% of the data to calibrate the models and 40% to validate them, according to the data selection process proposed by Medeiros et al. (2023).

Partial least squares discriminant analysis (PLS-DA) was performed by cross-validation using the software Chemoface version 1.65 (Nunes et al., 2012) to classify the wood density. The density categories for the correlation with PLS-DA were determined based on INDEA (2011); here,

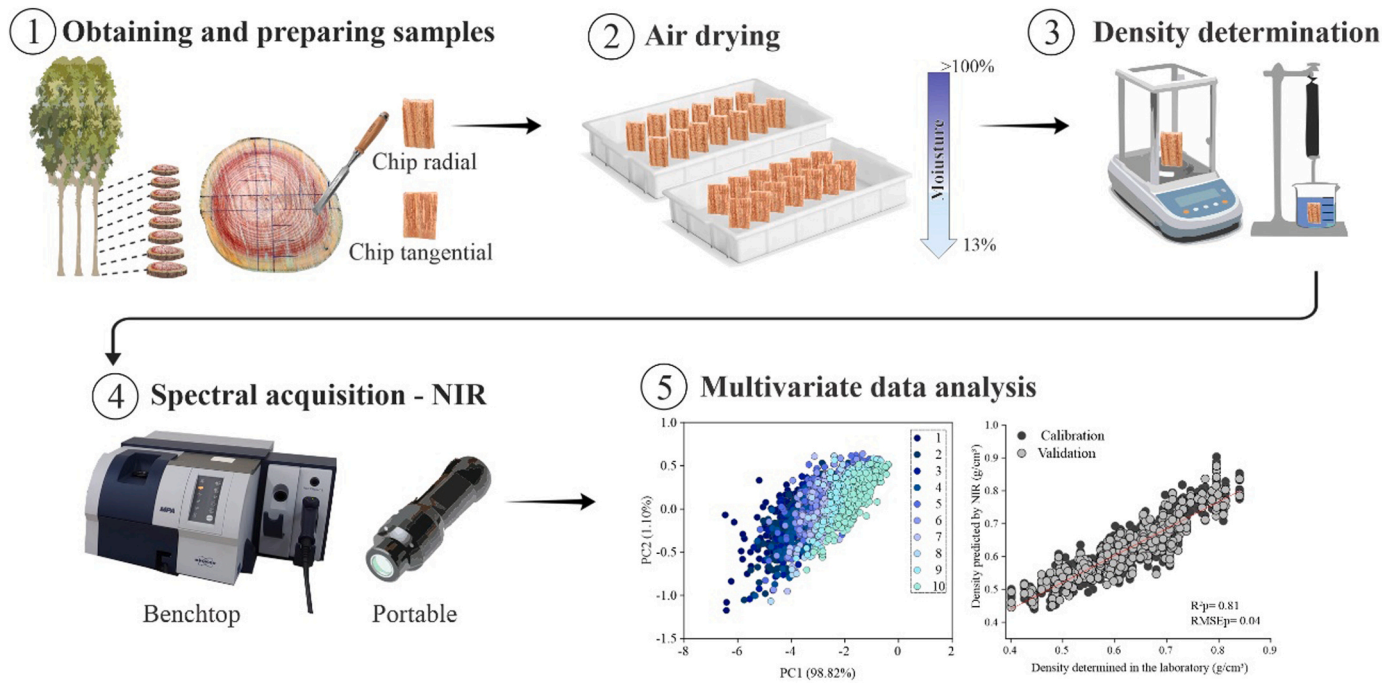

Fig. 1. Flowchart of the study stages.

very low density was considered to be < 0.40 g cm^{-3} , low density was considered to be between 0.40 and 0.55 g cm^{-3} , average density was considered to be between 0.55 and 0.75 g cm^{-3} and high density was considered to be > 0.75 g cm^{-3} .

The ratio of prediction deviation (RPD) was obtained as the ratio between the standard deviation of the values determined in the laboratory and the standard error of the cross-validation. The pretreatments of standard normal variation (SNV) and first and second Savitzky—Golay derivatives with 13 points and 3 polynomials were applied to the spectra to optimize the models. The PLS regression models were evaluated by the root mean square error (RMSE), coefficient of determination (R^2), ratio of prediction deviation (RPD), percentage of correct answers, and the effectiveness of the mathematical treatment.

3. Results and discussion

3.1. Monitoring of water desorption

The desorption of water in the wood showed uniformity according to the drying stages, even though each stage takes a different number of days to achieve the same water reduction (~10%). This uniformity is associated with the arrangement of the anatomical elements, chemical composition, and origin of the woody material. The maximum moisture values were approximately 100% for the radial chips (Fig. 2A) and approximately 130% for the chips obtained with tangential cuts (Fig. 2B). This variation in the moisture value per chip type could be explained by the order of production of the specimens; specifically, the tangential chips were prepared after the radial chips and were kept packaged for a longer time to avoid exposure to air. In the interval between the drying stages 9 and 10, an abrupt decrease in moisture was observed, which was expected due to obtaining the dry weight, in which the chips were subjected to artificial drying.

These desorption results by the drying step could be explained by the increase in the vapor pressure of the interior of the anatomical elements towards the atmospheric air. As a result, the mass flow of the residual free water was accelerated, which was more easily released until the fiber saturation point (FSP) was reached (Mascarenhas et al., 2020); here, the moisture of the wood was reduced by approximately 28–30% (Fredriksson et al., 2023). Hereafter, impregnation water was exclusively present and required more energy to be removed because the

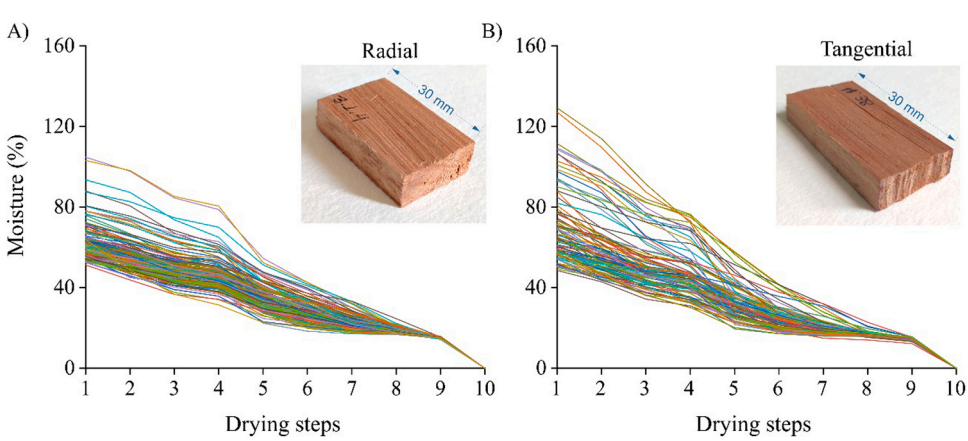

Fig. 2. Moisture reduction of the *Eucalyptus grandis* wood chips obtained from sections in the radial (A) and tangential (B) planes.

water-cellulose hydrogen bonds, which are stronger than the water—-water bonds, needed to be broken to promote the diffusion of water vapor through the layers of the cell wall.

Specifically, in addition to the different moisture levels that wood can present, the mechanisms of free water and impregnation water need to be considered as a variation factor for density estimates since the types of electrostatic interactions between the molecules and the hydroxyl groups of cellulose and hemicelluloses are distinct (Thybring and Fredriksson, 2021; Murr, 2022); for example, these interactions can influence the spectral signatures obtained with NIR.

This trend was reported by Amaral et al. (2020), who determined the *Eucalyptus* wood moisture content (approximately 80%) and observed the variations in the correlation factors with the spectral data. The water desorption patterns observed in this study were in agreement with other studies performed with wood and wood derivatives (Moretti et al., 2020; Lima et al., 2022a; Medeiros et al., 2023).

The amplitude of the moisture gradient is important for the prediction of the basic density of wood since the statistical models are trained to cover different moisture conditions in the same sample or different samples of the wood under study. Thus, the fitted model becomes more robust in predicting this property in woods with different moisture contents. According to Honorato et al. (2007), the addition of different sources of information in the data matrix causes the results to be more realistic and has greater applicability in the industrial environment.

3.2. Spectral signatures in the NIR

The chips obtained from the tangential and radial planes showed similar mean spectral profiles at different moisture levels (Fig. 3A). The minimum absorbance observed was 0.3, and the maximum was 0.9 for the benchtop instrument, indicating a low influence from the wood surface in the spectral acquisition.

Based on the analysis of the spectral signatures by type of instrument, the portable NIR had the lowest absorbance values, ranging from 0.1 to 0.4, both in the average signatures by type of surface (Fig. 3A) and in the signatures by drying step (Fig. 3B); this result was reasonable due to the type of lamp, luminous power, radiation intensity and acquisition technology (optical system), which were different from benchtop instrument; the benchtop system obtained spectral acquisition by an integrating sphere and had superior characteristics in the emission of electromagnetic radiation and the wavelength sweep.

From Fig. 3B, the absorbance in the NIR spectra decreased as the water desorption occurred in the wood; this process started at the saturated condition (step 1), reached equilibrium with the environment (step 9), and ended in the anhydrous condition (step 10), with a total of 272 spectra per drying step. This behavior of the signatures according to the water content was in agreement with the results found by Medeiros et al. (2023), who analyzed the desorption of water in cellulosic pulp with a benchtop NIR instrument.

The main absorbance peaks were in the waveband of 6800 cm^{-1} in the spectra from the benchtop NIR instrument and in the waveband of 5200 cm^{-1} in the spectra from the portable instrument. These spectral regions were related to the variation in moisture in the wood. According to Nisgoski et al. (2016), Costa et al. (2019), and Amaral et al. (2020), moisture intensified the interaction of electromagnetic radiation with the vibrations of hydroxyl groups, increasing the absorbance and information content of the material. For this reason, the absorbance decreased in increasing order of the drying steps in the spectral signatures.

The bands from 7000 cm^{-1} to 6800 cm^{-1} were attributed to the amount of cellulose, hemicelluloses, and lignin that corresponded to the main constituents of wood (Schwanninger et al., 2011). Specifically, the spectral signatures obtained for *Eucalyptus* wood under different moisture conditions were by reports in the literature for wood.

3.3. Principal component analysis

Similar to the spectral signatures, in the PCA scores obtained by first derivative spectra, the wood surfaces showed no visual difference regardless of the anatomical planes of the wood, since the variables obtained for each type of instrument remained superimposed (Fig. 4A and B). Corroborating these results, Costa et al. (2018) analyzed NIR spectra in the three anatomical planes of the wood and reported the same overlap of variables in the PCA plots considering the radial and tangential planes.

Although there are differences in the arrangement of cells in the different anatomical planes of wood, the chemical composition of wood does not significantly vary (Rowell, 2013). This may explain the results because the NIR spectra are associated with the vibrational patterns of the chemical groups present in the molecules that compose the wood.

However, in some cases, the greater exposure of a particular group of cells may influence the spectral signatures. For example, in woods that contain vessel elements filled with tyloses and the presence of radial and axial parenchyma with mucilaginous or oily content, peaks are potentially recorded in spectral bands more characteristic to a particular anatomical plane to the detriment of others (Braga et al., 2011; Karlinasari et al., 2021). In the present study, these effects were not observed, probably because the *Eucalyptus* wood contained heartwood and sapwood with low concentrations of extractives and other substances of secondary metabolism (Arisandi et al., 2023).

The chip drying stages followed a grouping trend according to moisture levels, starting in saturated conditions until reaching equilibrium with the environment (Fig. 4C and 4D). In the stage with more humid wood, greater dispersion of the samples was observed than in the

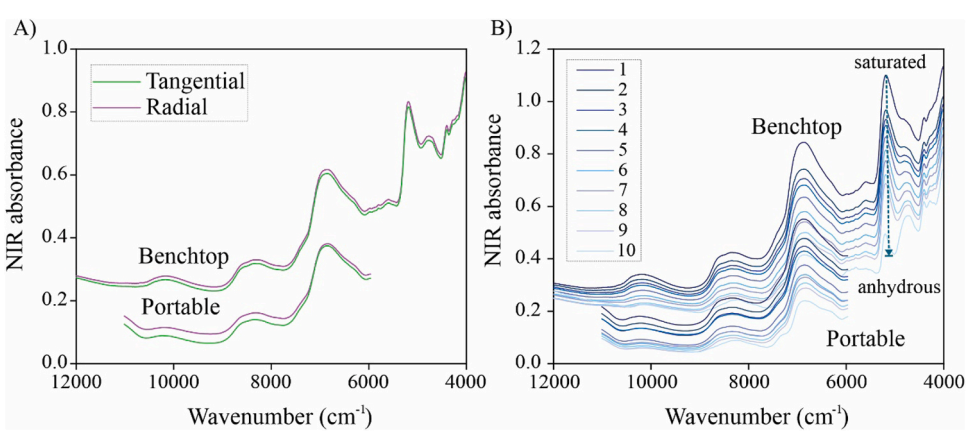

Fig. 3. Mean raw spectral signatures of the chips in different anatomical planes (Fig. 3A) and by drying stage (Fig. 3B) in *Eucalyptus grandis* wood obtained with benchtop and portable NIR instruments.

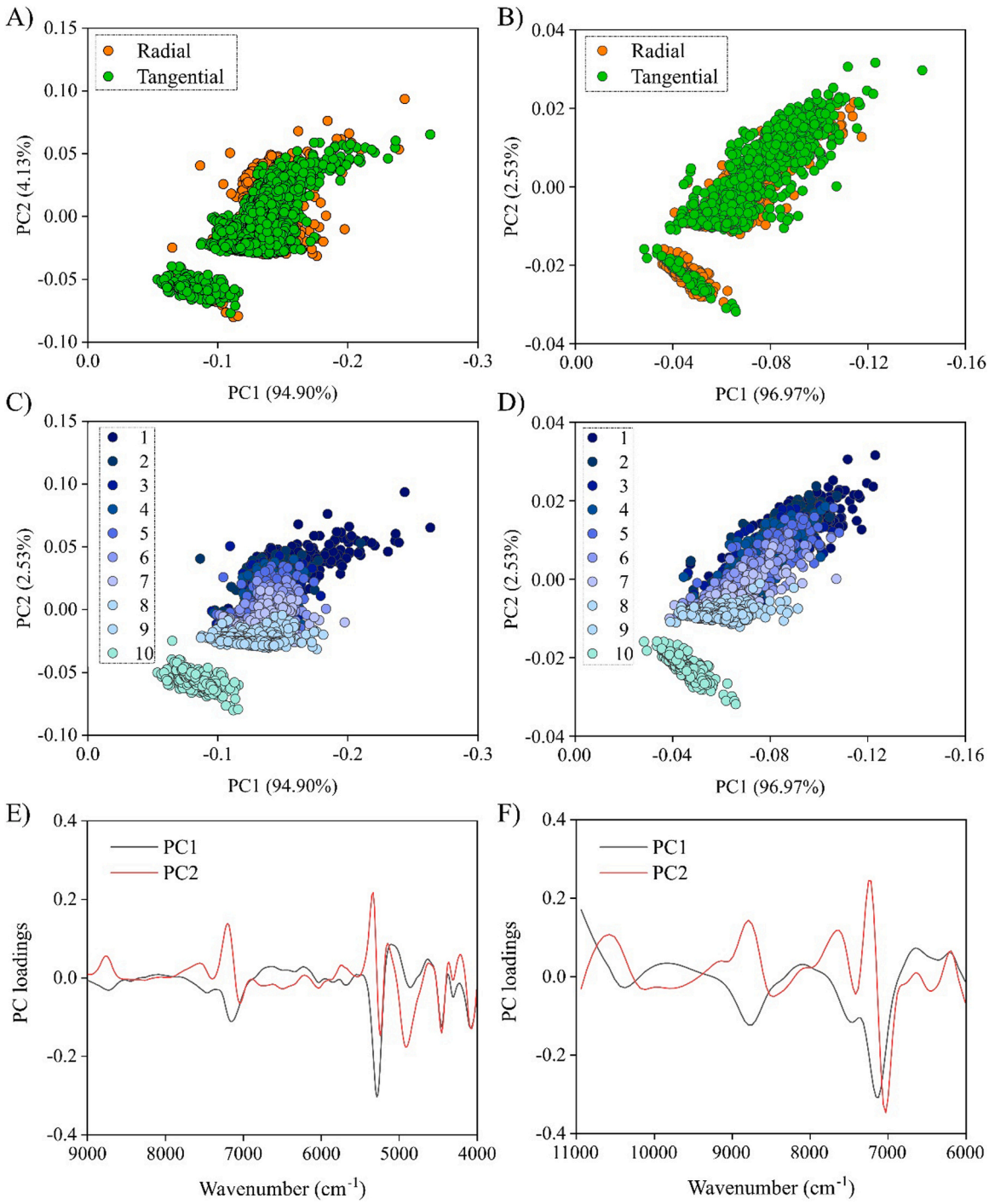

Fig. 4. PCA scores and PC loadings by wood surface and drying stage for the spectra treated with the first derivative from the benchtop NIR (A, C, and E) and the portable NIR instrument (B, D, and F).

drier stages. This trend was observed in the studies by Medeiros et al. (2023) in cellulosic pulp and by Amaral et al. (2020) in the examination of wood chips.

These variations were explained by the heterogeneity of the wood because, at moisture levels above the FSP, the amount of water varied depending on the inter- and intracellular spaces (Gezici-Koç et al., 2017). Since the examined samples were from different pith-bark and base-top positions, variations in the proportions of juvenile wood and mature wood, late wood and early wood, and, consequently, wood porosity were very likely. The development of models to discriminate the drying stage of wood is important in decision-making in forest-based industries because moisture directly interferes with several productive sectors, such as the production of pulp, furniture, panels, and charcoal.

In the principal component analysis loadings plots, the reflectance peaks were similar to those in the spectral signatures. Regarding the performance of the instruments, the portable NIR showed higher values than the benchtop NIR, in which the sum of principal component 1 and principal component 2 discriminated 99.50% of the information. In the benchtop NIR, 94.90% of the explanation of the data variation was represented by component 1, which was close to the portable instrument. Using PCA, Amaral et al. (2020) indicated that the discrimination of the drying steps in wood with benchtop NIR spectra was higher than

99.85%; these results were similar to those of this study. However, there are no reports of the use of portable NIR instruments for this purpose, highlighting the unprecedented nature of this information.

3.4. Partial least squares discriminant analysis

Basic density classification models for different wood moisture contents were fitted by PLS-DA based on the raw spectra collected from the NIR instruments (Table 1). In the confusion matrix, for the "very low" density class, no prediction success was achieved, regardless of the instrument used. For the "medium" class, success was obtained on the order of 93% and 94% for the benchtop NIR and portable NIR instruments, respectively.

A possible understanding of these results can potentially be based on the explanations by Kollmann and Côté (1968). The authors mentioned that low-density wood has cells with thinner cell walls and more pits. This, in turn, can induce multisurface reflectance, thus reducing the potential of electromagnetic radiation to capture the pertinent information. The presence of water can also influence this result because water vapor is capable of generating variations in the spectral signal due to the instability of the molecular geometry.

The success rate of the model developed with the benchtop instrument was 78%, which was slightly higher than that of the portable instrument with a 75% accuracy. Thus, the two instruments were able to classify the basic density of wood. Notably, the choice of instrument is influenced by the application environment and the nature of the sample, i.e., directly in the field or in the laboratory. In the study by Lima et al. (2022b), PLS-DA models for wood basic density classification were adjusted and their reported classification success rates were higher than 90%. However, the studied wood was at the equilibrium moisture content (~12%).

For the adjusted models to be promising for controlling the quality of raw materials in forestry companies, it would be necessary to expand the database with a greater range of variation, since the accuracy of the models was around 70%. Even so, although the statistical parameters in the "very low" and "low" moisture classes have shown inferior performance in predicting density, there is potential for using this tool to predict moisture in different packaging conditions of wood particles. This is in line with what was presented by those in the wood pulp and paper processing production chain, the ranges of density values that must be monitored are between 0.50 and 0.75 g cm^{-3} , falling within the range indicated in this study. Thus, even though the classification has less predictive capacity for the lower classes, our results fell within the moisture range that industries monitor wood in the pulping process and standardization of the final product.

3.5. Partial least squares regression

The models fitted by PLS-R to predict the basic density of the wood at different moisture levels exhibited coefficients of determination ranging from 0.77 to 0.86 in the different validations (Table 2).

In the spectra without mathematical treatment, the most appropriate statistical parameters were obtained for the radial surface on the benchtop instrument, with a coefficient of determination of 0.81 in the cross-validation. The error associated with the models followed similar values for RMSEcv and RMSEp, demonstrating uniformity in the data matrix. This consistency was observed in the cross-validation and independent validation, in which the correlation values did not differ from each other.

When applying mathematical treatment to the spectra, the models showed an increase in the coefficient of determination, and the tangential surface began to exhibit the best statistical values for both instruments and validation methods. The first derivative was the most efficient mathematical treatment, except for the radial surface in the portable instrument. In the performance deviation relationship (RPD), the models maintained low variation, with values between 2.20 and 2.45, meeting the predictions cited in the literature (Williams and Sobering, 1993; Fujimoto et al., 2007). The prediction coefficient of the models and the deviation performance ratio were selected according to the lowest error associated with the correlation for each piece of equipment and surface.

Regarding the type of instrument, the models showed low influence, but the portable NIR exhibited a slight reduction in the statistical parameters in certain correlation adjustments. According to Santos et al. (2020), this decrease in the performance of the models could be explained by the spectral readout area since the integrating sphere was approximately 10 mm in diameter, while the optical system had a point area, with less representation of the wood surface. However, both instruments were efficient in predicting the basic density of wood at different humidities.

Amaral et al. (2021) predicted the basic density of *Eucalyptus* wood at equilibrium moisture with original spectra in a benchtop NIR instrument; their data showed R^2cv= 0.70, RMSEcv= 0.4 and RPDcv= 1.83 on the radial surface of the wood, and the data treatment with the first derivative showed improvements in the models. Siesler et al. (2008) recommended the use of mathematical treatments in spectral data in the NIR to minimize noise in the spectral signal and indicated that the first derivative was one of the main treatments because it reduced the systematic displacement of the baseline.

Vimal and Dubey (2014) used NIR spectroscopy to estimate the basic density of *Eucalyptus tereticornis* wood in the green condition (30% moisture) and evaluated the spectral acquisition mode (integrating sphere and optical fiber) and the effect of the radial and tangential surface on the model calibration. The best coefficients of determination were obtained on the radial surface and on the integrating sphere, which corroborated the results of this study.

Fig. 5 shows the plots of the PLS-R validation of the data with first derivate mathematical treatment to predict the basic density of *Eucalyptus grandis* wood at different moisture levels, and the property correlation was performed with the values determined in laboratories via

Table 1
Confusion matrix of the partial least squares analysis for the classification of wood density at different moisture contents in the two NIR instruments.

Classification of wood density								
		Very low	Low	Mean	High	N of samples	%Success	Total
Real class								
Benchtop NIR Instrument								
Predicted class	Very low	0	30			30	0	78%
	Low		336	323		659	51	
	Mean		126	1664		1790	93	
	High			199	35	234	15	
Portable NIR Instrument								
Predicted class	Very low	0	30			30	0	75%
	Low		329	330		659	50	
	Mean		106	1684		1790	94	
	High			200	34	234	14	

Table 2
Statistical parameters of the PLS-R models to predict the basic density of *Eucalyptus grandis* wood at different moisture levels.

Instrument	Surface	Treatment	R^2cv	RMSEcv	R^2p	RMSEp	RPDcv
Benchtop	RD	untreated	0.817	0.038			
	TG		0.794	0.054	0.810	0.053	2.20
	RD	1°D	0.833	0.036	0.831	0.037	2.45
	TG		0.857	0.045			
	RD	2°D	0.798	0.040			
	TG		0.831	0.049			
	RD	SNV	0.797	0.040			
	TG		0.796	0.054			
Portable	RD	untreated	0.815	0.038	0.813	0.038	2.33
	TG		0.771	0.057			
	RD	1°D	0.780	0.041			
	TG		0.827	0.049	0.833	0.048	2.44
	RD	2°D	0.777	0.042			
	TG		0.815	0.051			
	RD	SNV	0.788	0.041			
	TG		0.815	0.050			

R^2c - coefficient of determination for calibration; RMSEc - root mean square error for calibration; R^2cv - coefficient of determination for cross-validation; RMSEcv - root mean square error for cross-validation; R^2p - coefficient of determination for prediction; RMSEP - root mean square error for prediction; RPDcv - the ratio of performance to deviation for cross-validation. RD – Radial; TG – Tangential. 1D - first derivative; 2D - second derivative; SNV - standard normal variate.

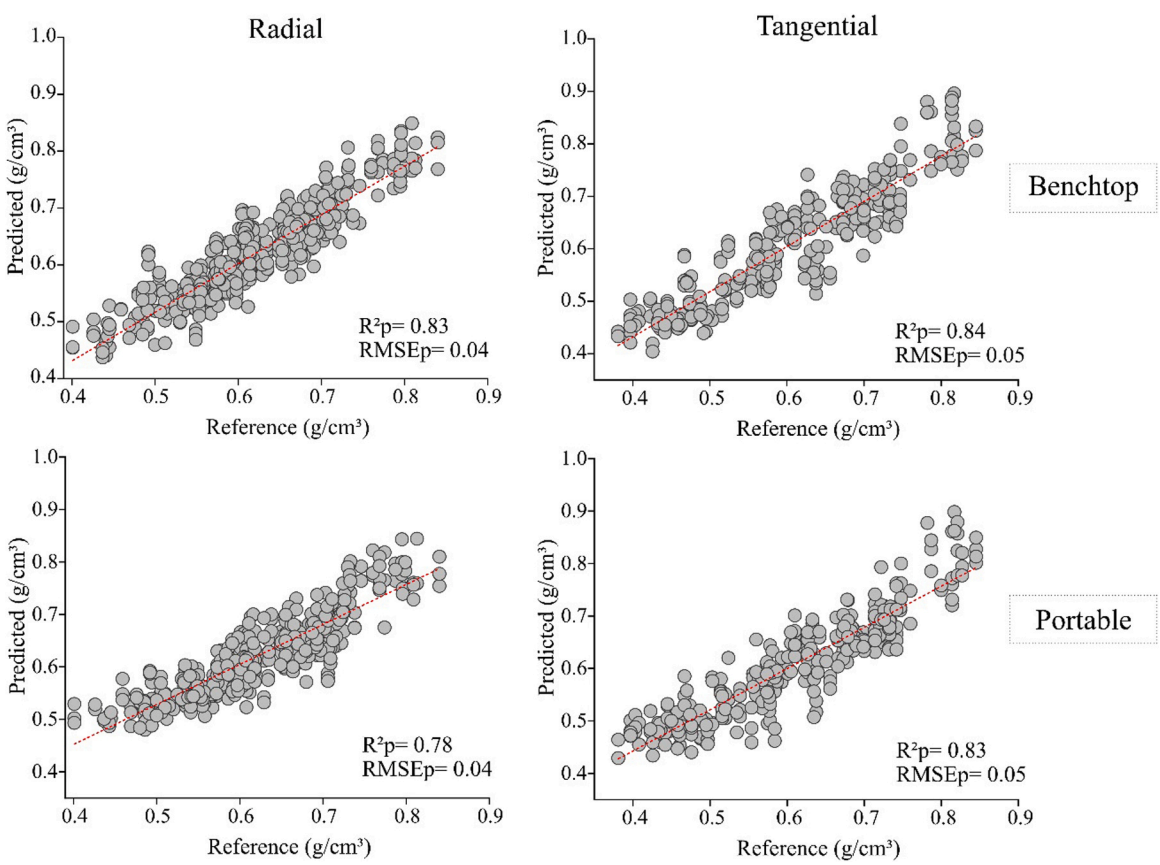

Fig. 5. Plot of the PLS-R validations treated with first derivative to predict the basic density at different moisture contents by type of instrument and wood surface.

conventional methods and predicted via NIR technology with the benchtop and portable instruments and the scattering trends for the radial and tangential surface of the wood.

Visually, the effect of the instrument and the wood surface was negligible; however, when analyzing the predicted values, a reduction in the coefficient of determination was observed on the radial surface with the benchtop and portable NIR. Costa et al. (2018) reported that the spectral reading on the radial surface included information from several years of wood formation, while in the tangential direction of the shaft, the representativeness of the wood formation was from a shorter period, which agreed with our model results. In the study by Costa et al. (2019), models developed with a benchtop NIR instrument to predict wood moisture in different water proportions also showed adequate prediction values, corroborating our basic density results for wood.

Based on the analysis of the coefficient of determination of the PLS-R models by drying stage, the wood moisture did not affect the R^2 values of the cross and independent validations, regardless of the instrument or surfaces, reinforcing the potential of NIR technology for industrial use (Fig. 6). The error associated with the PLS-R models showed uniform variation, with values between 0.02 and 0.06 g/cm^3, in the cross-

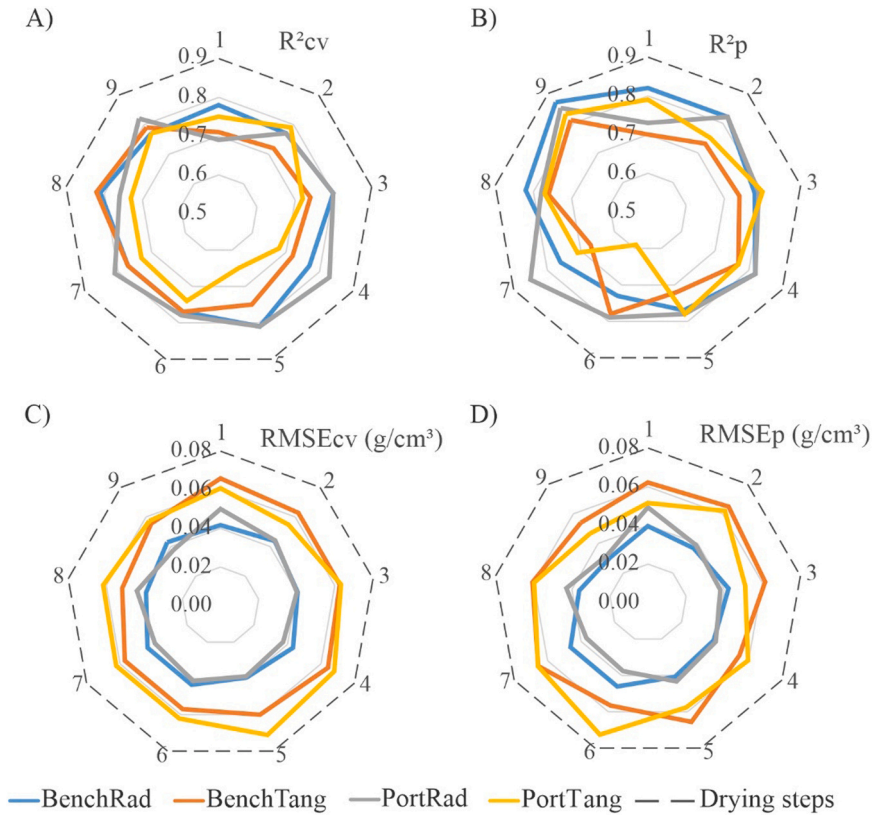

Fig. 6. Graphs of the prediction of the basic density per drying stage (stage 1 - wetter to stage 9 - drier) in different surfaces and instruments in the cross-validation (A) and in the independent validation (B) and their respective errors (C and D).

validation and the prediction.

The radial surface maintained the best statistical performance in all models, and the tangential surface presented reduced values. This answers one of the hypotheses outlined in this research, considering that for the wood under study, the anatomical plane can contribute to improving estimates. This can be seen more clearly when analyzing the most significant statistical parameters observed in drying step 9; here, the chips were at equilibrium moisture content with the environment (~12%). However, the difference in values between the drying stages was practically insignificant because the robustness of these models was suitable for practical field and laboratory applications.

Arriel et al. (2019) estimated the basic density of *Eucalyptus* wood at equilibrium moisture using benchtop NIR and reached $R^2cv = 0.55$ and RMSEcv= 0.26 for the spectra treated with the first derivative and collected on the transverse surface. In the same way, Costa et al. (2018) predicted the basic density with $R^2p = 0.73$ and $R^2p = 0.76$ on the tangential and radial surfaces, respectively.

Thus, the radial surface had the most reliable results, in agreement with the results of this study. This could be explained by the fact that the radial section of *Eucalyptus* wood was characterized by greater exposure of the fiber mass, which was highly correlated with wood density (Pirralho et al., 2014). The tangential section had part of its exposed area covered by voids in the lumens of the radial parenchyma, causing discontinuity of the woody mass. Thus, this discontinuity in the tangential section could potentially cause a reduction in the spectral interaction with the cell wall of the fibers.

By observing the global model plot and its β-coefficients for the basic density of *Eucalyptus grandis* wood in the NIR instrument, verification of the predictive accuracy for the models was fairly possible, and the model accuracy in different wood moistures and surfaces was maintained (Fig. 7).

In the β-coefficients of the global model, the most significant reflectance peaks were in the band 5500 cm^{-1} and the range of 6800–7200 cm^{-1}, for benchtop and portable equipment, respectively. Medeiros et al. (2023) developed a global model for the prediction of cellulosic pulp moisture at different moisture contents and pulp types using benchtop NIR, and the results were also promising, with an R^2 of 0.95, RMSEp of 0.1 g/cm^3 and β-coefficients with peaks in the band 5500 cm^{-1}, with reflectance NIR values ranging from − 1.50–2.25. Honorato et al. (2007) report that the global model enhanced the validation ability to predict the property of interest due to possible variations in data analysis.

Visually, the PLS-R correlations of the instruments were similar, with equivalent linear trend adjustments and minimal differences in the prediction values. Thus, in the results of the present study, the proposed objectives were achieved because the instruments demonstrated equivalent performance, with the main difference being in their handling. Thus, the benchtop and portable NIR instruments could be used to estimate the basic density considering different moisture contents and wood surfaces.

It is worth noting that this study has limitations regarding species diversity, as in this work only *Eucalyptus grandis* wood was considered. Additionally, the storage and drying conditions of the wood under study were standardized, unlike what occurs in sawmills and wood storage yards, where the raw material is eventually exposed to photodegradation, oxidation, and deterioration by xylophagous agents.

Therefore, it is necessary to carry out more studies considering the sources of variation to better understand the influence of these factors on the predictions of wood technological parameters, especially density. Considering that this parameter varies between species, and between different positions of the trunk (pith-bark and base-top), it is influenced by management and silvicultural treatments, varies between growth rings, and is also influenced by nutritional parameters and water availability. This, in turn, will reflect different spectral responses that can influence the obtaining of predictive models from NIR spectroscopy.

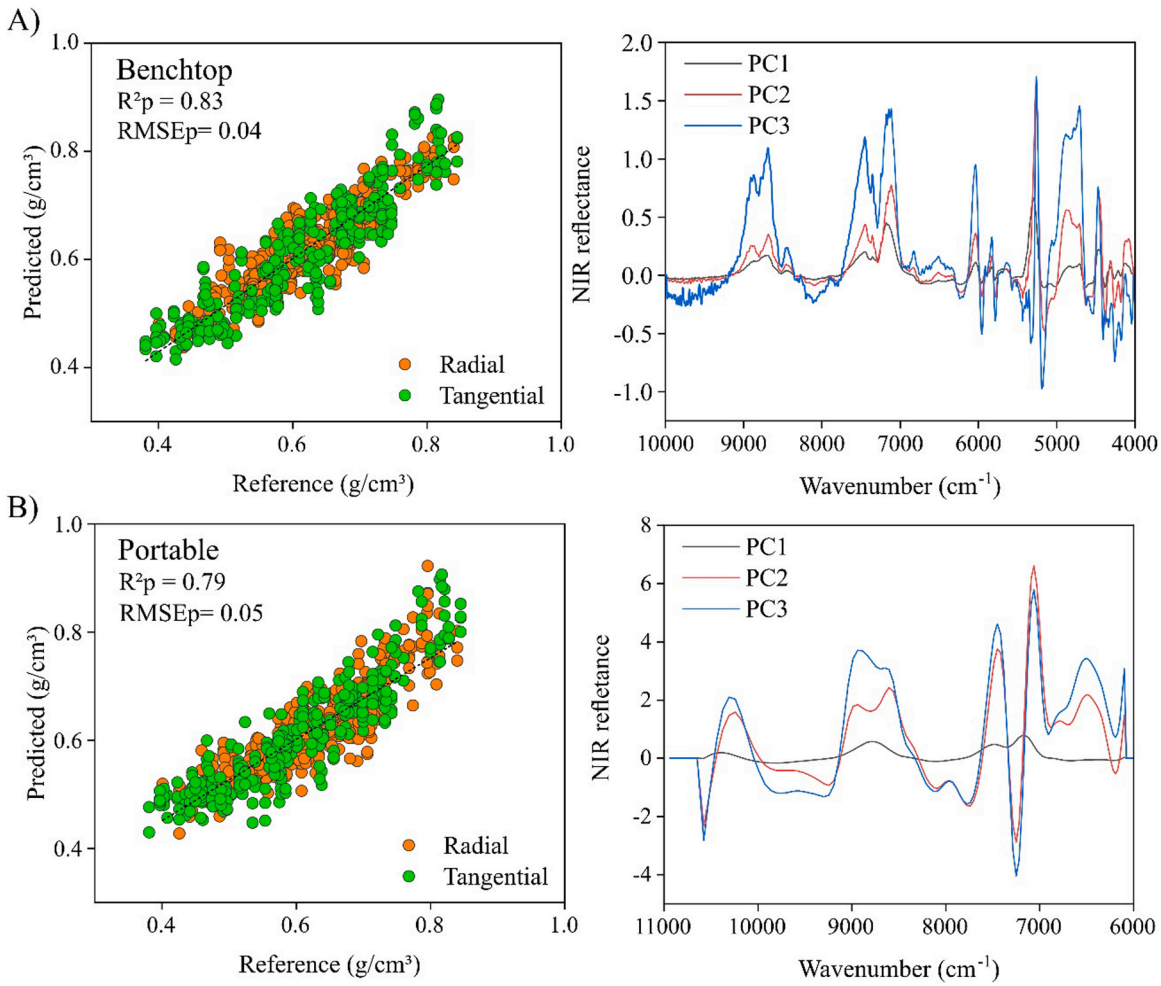

Fig. 7. Global model for the basic density of *Eucalyptus grandis* wood in benchtop (A) and portable (B) NIR instruments, with spectra treated with first derivative.

4. Conclusion

The PLS-R models developed with the NIR spectra showed adequate coefficients of determination (R^2 of 0.77–0.85) to predict the basic density of *Eucalyptus grandis* wood at different moisture levels, and the performances of the models were not affected by moisture content. Thus, based on these models, the basic density could be fairly estimated in woods recently cut or after the desorption of water in industrial yards, contributing to the optimization of production processes.

The radial surface of the sample, with the spectra without mathematical treatment, was the most suitable for spectral collection, regardless of the NIR instrument used. The instruments showed equivalent application potential. However, the portable NIR instrument has a lower cost, and its operation is more dynamic than that of the benchtop instrument. Thus, based on the results from this study, the acquisition of reliable estimates with different NIR spectrometers was possible.

CRediT authorship contribution statement

Gomes Jhennyfer Nayara Nogueira: Methodology, Visualization. **Batista Felipe Gomes:** Methodology, Software, Visualization, Writing – review & editing. **Medeiros Dayane Targino de:** Conceptualization, Data curation, Methodology, Writing – original draft. **Chaix Gilles:** Data curation, Formal analysis, Supervision, Writing – review & editing. **Hein Paulo Ricardo Gherardi:** Data curation, Funding acquisition, Supervision, Writing – review & editing. **Mascarenhas Adriano Reis Prazeres:** Formal analysis, Supervision, Visualization, Writing – review & editing. **Pimenta Emanuella Mesquita:** Investigation, Visualization.

Declaration of Competing Interest

The authors declare that they have no known competing financial interests or personal relationships that could have appeared to influence the work reported in this paper.

Data Availability

The authors do not have permission to share data. Data will be made available on request.

Acknowledgments

The authors thank the Wood Science and Technology Graduation Program (DCF/ UFLA, Brazil) and Núcleo de Estudos em Madeira (NEMAD, UFLA) along with the AGAP joint research unit and Chem-House group at CIRAD in Montpellier (France) for all the support for this study. This project was financed in part by the Coordenação de Aperfeiçoamento de Pessoal de Nível Superior – Brazil (CAPES) – Finance Code 001, by the Conselho Nacional de Desenvolvimento Científico e Tecnológico (CNPq: grants n. 406593/2021–3) and by Fundação de Amparo à Pesquisa do Estado de Minas Gerais (FAPEMIG, APQ-00742-23). P.R.G. Hein was supported by CNPq grants (process no. 309620/2020–1).

References

Amaral, E.A., Santos, L.M., Costa, E.V., Trugilho, P.F., Hein, P.R., 2020. Estimation of moisture in wood chips by near infrared spectroscopy. Maderas Cienc. Y. Technol. 22 (3), 291–302. https://doi.org/10.4067/S0718-221×2020005000304.

Amaral, E.A., Santos, L.M., Hein, P.R., Costa, E.V., Rosado, S.C.S., Trugilho, P.F., 2021. Evaluating basic density calibrations based on NIR spectra recorded on the three wood faces and subject to different mathematical treatments. New Zealand Journal of Forestry Science 51 (2), 1–6. https://doi.org/10.33494/nzjfs512021x100x.

Arisandi, R., Marsoem, S.N., Sutapa, J.P.G., Lukmandaru, G., 2023. Heartwood formation and its relationship with basic density and green moisture content of young small-leaf mahogany trees. South. For.: A J. For. Sci. 85 (1), 26–39. https://doi.org/10.2989/20702620.2023.2180453.

Arriel, T.G., Ramalho, F.M.G., Lima, R.A.B., Sousa, K.I.D., Hein, P.R.G., Trugilho, P.F., 2019. Developing near-infrared spectroscopic models for predicting the density of *Eucalyptus* wood based on indirect measurement. Cerne 25 (3), 294–300. https://doi.org/10.1590/01047760201925032646.

ASTM. Standard, 2017a. ASTM D5536–17: Standard Practice for Sampling Forest Trees for Determination of Clear Wood Properties.

ASTM. Standard, 2017b. ASTM D2395–17: Standard Test Methods for Density and Specific Gravity (Relative Density) of Wood and Wood-Based Materials.

Braga, J.W.B., Pastore, T.C.M., Coradin, V.T.R., Camargos, J.A.A., Silva, A.R., 2011. The use of near-infrared spectroscopy to identify solid wood specimens of *Swietenia macrophylla* (Cites Appendix II). IAWA J. 32 (2), 285–296.

Costa, E.V.S., Rocha, M.F.V., Hein, P.R.G., Amaral, E.A., Santos, L.M.D., Brandão, L.E.V.S., Trugilho, P.F., 2018. Influence of spectral acquisition technique and wood anisotropy on the statistics of predictive near-infrared–based models for wood density. J. Infrared Spectrosc. 26 (2), 106–116. https://doi.org/10.1177/0967033518757070.

Costa, L.R., Tonoli, G.H.D., Milagres, F.R., Hein, P.R.G., 2019. Artificial neural network and partial least square regressions for rapid estimation of cellulose pulp dryness based on near-infrared spectroscopic data. Carbohydr. Polym. 224, 115186 https://doi.org/10.1016/j.carbpol.2019.115186.

Fredriksson, M., Rüggberg, M., Nord-Larsen, T., Beck, G., Thybring, E.E., 2023. Water sorption in wood cell-walls-data exploration of the influential physicochemical characteristics. Cellulose 30 (3), 1857–1871. https://doi.org/10.1007/s10570-022-04973-0.

Fujimoto, T., Kurata, Y., Matsumoto, K., Tsuchikawa, S., 2007. Application of near-infrared spectroscopy for estimating wood mechanical properties of small clear and full-length lumber specimens. J. Infrared Spectrosc. 16 (6), 529–537. ⟨https://opg.optica.org/jnirs/abstract.cfm?URI=jnirs-16-6-529⟩.

Gezici-Koç, O., Erich, S.F., Huinink, H.P., Ven, L.G.J., Adan, O.C.G., 2017. Bound and free water distribution in wood during water uptake and drying as measured by 1D magnetic resonance imaging. Cellulose 24, 535–553. https://doi.org/10.1007/s10570-016-1173-x.

Hein, P.R.G., Campos, A.C.M., Trugilho, P.F., Lima, J.T., Chaix, G., 2009. Near infrared spectroscopy for estimating wood basic density in *Eucalyptus urophylla* and *Eucalyptus grandis*. Cerne 15 (2), 133–141.

Honorato, F.A., Barros Neto, B.D., Martins, M.N., Galvão, R.K.H., Pimentel, M.F., 2007. Transferência de calibração em métodos multivariados. Quím. Nova 30 (5), 1301–1312. https://doi.org/10.1590/S0100-40422007000500044.

IBÁ. Brazilian Tree Industry., 2022. Annual Report 2022. Avaible in: (https://www.iba.org/datafiles/publicacoes/relatorios/relatorio-anual-iba2022compactado.pdf). Access: 23 Jun 2023.

INDEA. Institute of Agricultural Defense of the State of Mato Grosso., 2011. Basic notions of anatomy and macroscopic identification of wood. Cuiabá, 1–12.

Karlinasari, L., Noviyanti, N., Purwanto, Y.A., Majiidu, M., Dwiyanti, F.G., Rafi, M., Damayanti, R., Harnelly, E., Siregar, I.Z., 2021. Discrimination and determination of extractive content of ebony (*Diospyros celebica* Bakh.) from celebes island by near-infrared spectroscopy. Forests 12 (6), 1–11. https://doi.org/10.3390/f12010006.

Kollmann, F., Côté, J.R., 1968. Principles of wood science and technology: I Solid Wood.

Lima, M.D.R., Trugilho, P.F., Bufalino, L., Júnior, A.F.D., Ramalho, F.M.G., Paula Protásio, T., Hein, P.R.G., 2022b. Efficiency of near-infrared spectroscopy in classifying Amazonian wood wastes for bioenergy generation. Biomass Bioenergy 166, 106617. https://doi.org/10.1016/j.biombioe.2022.106617.

Lima, M.F.M., Mascarenhas, A.R.P., Pereira, B.L.C., Susin, F., Silva, G.A.O., Stangerlin, D.M., 2022a. Experimental characterization of density, defects, and drying kinetics of three Amazonian wood species: *Astronium lecointei, Dinizia excelsa, and Hymenolobium heterocarpum*. Wood Mater. Sci. Eng. 18 (4), 1264–1274. https://doi.org/10.1080/17480272.2022.2125339.

Mascarenhas, A.R.P., Ghilardi, D.S., Melo, R.R., 2020. Geotechnologies applied to seasonal zoning of equilibrium moisture content of timber in Rondonia, Brazil. Anuário do Inst. De. Geociênc. 43 (2), 119–127. https://doi.org/10.11137/2020_2_119_127.

Medeiros, D.T., Ramalho, F.M.G., Batista, F.G., Mascarenhas, A.R.P., Chaix, G., Hein, P.R.G., 2023. Water desorption monitoring of cellulose pulps by NIR spectroscopy. Ind. Crops Prod. 192, 115989 https://doi.org/10.1016/j.indcrop.2022.115989.

Moretti, S.D.A., Santos, C.M.M., Mascarenhas, A.R.P., Oliveira, J.P., Anjos, S.P., 2020. Evaluation of the outdoor drying process of jatoba wood in the Amazon. Research 9 (9), e252997258. https://doi.org/10.33448/rsd-v9i9.7258.

Murr, A., 2022. Water vapor sorption and moisture transport in and across fibre direction wood. Cellulose 29, 4135–4152. https://doi.org/10.1007/s10570-022-04520-x.

Nisgoski, S., Klock, U., Batista, F.R.R., Schardosin, F.Z., Consalter, R., Motta, A.C.V., 2016. Uso do NIR na discriminação de árvores em diferentes adubações com base nos espectros da madeira e da casca. Rev. Ciência da Madeir. (Braz. J. Wood Sci.) 7 (2), 100–110. https://doi.org/10.12953/2177-6830/rcm.v7n2p100-110.

Nunes, C.A., Freitas, M.P., Pinheiro, A.C.M., Bastos, S.C., 2012. Chemoface: a novel free user-friendly interface for chemometrics. J. Braz. Chem. Soc. 23, 2003–2010. https://doi.org/10.1590/S0103-50532012005000073.

Pirralho, M., Flores, D., Sousa, V.B., Quilhó, T., Knapic, S., Pereira, H., 2014. Evaluation of paper making potential of nine *Eucalyptus* species based on wood anatomical features. Ind. Crops Prod. 54, 327–334. https://doi.org/10.1016/j.indcrop.2014.01.040.

Ramalho, F.M., Andrade, J.M., Hein, P.R., 2018. Rapid discrimination of wood species from native forest and plantations using near infrared spectroscopy. For. Syst. 27 (2) https://doi.org/10.5424/fs/2018272-12075 e008-e008.

Rowell, M.R., 2013. Handbook of Wood Chemistry and Wood Composites.

Rosso, S., Muniz, G.I.B.D., Matos, J.L.M.D., Haselein, C.R., Hein, P.R.G., Lopes, M.D.C., 2013. Predição da massa específica de *Eucalyptus grandis* W. Hill ex Maiden por espectroscopia no infravermelho próximo. Cerne 19 (4), 647–652. https://doi.org/10.1590/S0104-77602013000400015.

Sandak, J., Sandak, A., Meder, R., 2016. Assessing trees, wood and derived products with near infrared spectroscopy: hints and tips. J. Infrared Spectrosc. 24 (6), 485–505. ⟨https://opg.optica.org/jnirs/abstract.cfm?URI=jnirs-24-6-485⟩.

Santos, L.M., Amaral, E.A., Nieri, E.M., Costa, E.V.S., Trugilho, P.F., Calegário, N., Hein, P.R.G., 2020. Estimating wood moisture by near infrared spectroscopy: testing acquisition methods and wood surfaces qualities. Wood Mater. Sci. Eng. 16 (5), 336–343. https://doi.org/10.1080/17480272.2020.1768143.

Schwanninger, M., Rodrigues, J.C., Fackler, K., 2011. A review of band assignments in near infrared spectra of wood and wood components. J. Infrared Spectrosc. 19 (5), 287–308. https://doi.org/10.1255/jnirs.955.

Sheppard, N., Willis, H.A., Rigg, J.C., 1985. Commission on molecular structure and spectroscopy and commission on quantities and units in clinical chemistry. Pure Appl. Chem. 57 (1), 105–120.

Siesler, H.W., Kawata, S., Heise, H.M., Ozaki, Y. (Eds.), 2008. Near-Infrared Spectroscopy: Principles, Instruments, Applications. John Wiley & Sons.

Thybring, E.E., Fredriksson, M., 2021. Wood modification as a tool to understand moisture in wood. Forests 12 (3), 1–18. https://doi.org/10.3390/f12030372.

Vimal, K., Aasheesh, R., Dubey, Y.M., 2014. Enhancing the applicability of near infrared spectroscopy for estimating specific gravity of green timber from *Eucalyptus tereticornis* by developing composite calibration using both radial and tangential face of wood. Eur. J. Wood Wood Prod. 72 (1), 11–20. https://doi.org/10.1007/s00107-013-0742-z.

Williams, P.C., Sobering, D.C., 1993. Comparison of commercial near infrared transmittance and reflectance instruments for analysis of whole grains and seeds. J. Infrared Spectrosc. 1 (1), 25–32. https://doi.org/10.1255/jnirs.3.